chemistry

Article

Production of Alkyl Levulinates from Carbohydrate-Derived Chemical Intermediates Using Phosphotungstic Acid Supported on Humin-Derived Activated Carbon (PTA/HAC) as a Recyclable Heterogeneous Acid Catalyst

Nivedha Vinod [ID] and Saikat Dutta *[ID]

Department of Chemistry, National Institute of Technology Karnataka (NITK), Mangaluru 575025, Karnataka, India
* Correspondence: sdutta@nitk.edu.in

Abstract: This work reports a straightforward and high-yielding synthesis of alkyl levulinates (ALs), a class of promising biofuel, renewable solvent, and chemical feedstock of renewable origin. ALs were prepared by the acid-catalyzed esterification of levulinic acid (LA) and by the alcoholysis of carbohydrate-derived chemical platforms, such as furfuryl alcohol (FAL) and α-angelica lactone (α-AGL). Phosphotungstic acid (PTA) was chosen as the solid acid catalyst for the transformation, which was heterogenized on humin-derived activated carbon (HAC) for superior recyclability. Using HAC as catalyst support expands the scope of valorizing humin, a complex furanic resin produced inevitably as a side product (often considered waste) during the acid-catalyzed hydrolysis/dehydration of sugars and polymeric carbohydrates. Under optimized conditions (150 °C, 7 h, 25 wt.% of 20%PTA/HAC-600 catalyst), ethyl levulinate (EL) was obtained in an 85% isolated yield starting from FAL. Using the general synthetic protocol, EL was isolated in 88% and 84% yields from LA and α-AGL, respectively. The 20%PTA/HAC-600 catalyst was successfully recovered from the reaction mixture and recycled for five cycles. A marginal loss in the yield of ALs was observed in consecutive catalytic cycles due to partial leaching of PTA from the HAC support.

Keywords: alkyl levulinate; levulinic acid; furfuryl alcohol; heterogeneous catalyst; heteropoly acid; renewable synthesis

1. Introduction

The past two decades have seen exponential growth in biorefinery research with the central goal of making the organic chemical manufacturing industry more sustainable by reducing dependence on exhaustible, fossilized feedstock [1]. Dedicated research has been undertaken to identify biomass components and specific feedstocks that can be catalytically converted into the drop-in replacement of existing petrochemicals as well as their renewable substitutes [2]. Cellulose and hemicellulose together make up around 70 wt.% of dry non-food lignocellulosic biomass and these polymeric carbohydrates have received serious attention from the academic and industrial community as a renewable source of biogenic carbon for synthesizing organic fuels, chemicals, and polymers [3]. The carbohydrate fraction in the algal biomasses (freshwater and marine) is also significant [4]. An established strategy for the chemical-catalytic value addition of these polymeric carbohydrates is through acid-catalyzed hydrolysis, where the sugar molecules formed as intermediates undergo dehydration reaction into furanic chemical platforms under appropriate conditions [5]. Xylose, an abundant pentose sugar in hemicellulose, becomes dehydrated into furfural (FF) [6]. Analogously, cellulose-derived glucose is dehydrated into 5-(hydroxymethyl)furfural (HMF) [7]. The acid-catalyzed transformations are astounding from a green chemistry perspective since water is produced as the sole innocuous

byproduct, and no stoichiometric reagent is warranted. The production of FF from biomass has been commercialized, and many of its derivatives have established markets [8]. For example, furfuryl alcohol (FAL), produced by the partial reduction of FF under catalytic hydrogenation conditions, has major applications in the paint and resin industry [9]. The production of HMF and its derivatives have a significant presence in the literature and thousands of publications are added every year on their production, derivative chemistry, and applications [10]. Not surprisingly, FF and HMF have been recognized globally as the most promising carbohydrate-derived renewable chemical platforms for synthesizing products of commercial interest [11]. HMF and FAL can be transformed into levulinic acid (LA) by hydrolysis at elevated temperatures under acid catalysis [12]. LA has received significant attention as a carbohydrate-derived chemical platform to synthesize numerous renewable chemicals of commercial significance [13]. Commercial ventures, such as the Biofine process, demonstrated the direct transformation of lignocellulose into LA in acceptable yields and promising production costs [14]. Alkyl levulinates (ALs) can be produced from LA, FAL, LA-derived α-angelica lactone (α-AGL), and even directly from carbohydrates by reacting with C1-C4 monohydric alcohols under acid-catalyzed esterification and alcoholysis [15]. ALs have garnered immense attention due to their existing and emerging applications as biofuels, green solvents, and chemical intermediates for downstream synthetic value addition [16]. An acid catalyst of some sort is routinely used for these transformations, including mineral acids, solid Brønsted and Lewis acids (supported and unsupported), acidic resins, and acidic ionic liquids [15]. Even though several efficient catalysts have been developed over the years, the search continues for more efficient (e.g., high activity, good selectivity), inexpensive, recyclable, and eco-friendly catalyst candidates for synthesizing ALs under economically amenable reaction parameters. Catalysts that function equally well with multiple feedstocks to form ALs following a general synthetic protocol are rather limited.

In this regard, heteropoly acids (HPAs), the protonated versions of heteropolymetalates, are increasingly used in chemical-catalytic biomass value-addition pathways and sustainable chemistry [17–19]. HPAs are considered a greener alternative to mineral acids and many other solid acid catalysts due to various advantageous properties, such as strong Brønsted acidity, low corrosivity, no volatility, high thermal stability, and tunable solubility [20]. HPAs have already been explored as an acid catalyst in synthesizing ALs, and the works have recently been reviewed [21]. HPAs are often heterogenized by partially replacing the protons with suitable cations (e.g., Cs^+, quaternary ammonium) or supported on solid materials (e.g., SiO_2, zeolite) to assist their convenient recovery from the reaction mixture and recycling [22]. Carbon is a promising heterogeneous supporting material for solid acids and metal catalysts due to its chemical resistance in acidic or basic reaction media, high thermal stability, low cost, and tailored morphology, among others [23,24]. Interestingly, HPAs supported on activated carbon have also been reported for synthesizing ALs [25,26].

Humin is a complex furanic resin that forms as a side product when sugars and polymeric carbohydrates are dehydrated into FF, HMF, and LA [27]. Recent studies have attempted to understand the mechanistic details of its formation so that this unwanted side product can be minimized [28]. Humin is typically combusted to produce process heat for other biorefinery processes, but more profitable uses of humin, such as renewable materials and catalyst support, are being explored [29]. A carbonaceous solid acid catalyst derived from humin (produced during the dehydration of glucose) has been used as an efficient acid catalyst with a high surface area for synthesizing ALs and diesel fuel precursors from LA and FF [30]. Humin-derived carbon could prove to be a promising catalyst support for HPAs for use as a heterogeneous acid catalyst in synthesizing ALs from carbohydrate-derived chemical intermediates. Value-adding humin as a supporting material for catalysts would be beneficial for improving the commercial appeal of an integrated biorefinery.

In this work, phosphotungstic acid (PTA, $H_3PW_{12}O_{40}$) has been supported on humin-derived activated carbon (HAC) to heterogenize the Keggin-type HPA. Humin used in this

work was obtained by the acid-catalyzed dehydration of xylose into FF. The PTA/HAC-600 was then used as a heterogeneous acid catalyst for the alcoholysis of FAL with C1-C4 mono-hydric alcohols in a batch-type sealed glass reactor. Moreover, other chemical intermediates such as LA and α-AGL have also been successfully converted into ALs in excellent isolated yields (Scheme 1). The PTA/HAC-600 catalyst was recovered from the reaction medium by centrifugation and successfully recycled for several cycles. The PTA/HAC-600 catalysts (fresh and recycled) were characterized by Fourier Transform Infrared Spectroscopy (FTIR), Powder X-ray Diffraction (PXRD), Field Emission Scanning Electron Microscopy-Energy Dispersive X-ray Analysis (FESEM-EDX), NH_3-Thermal Conductivity Detector (TCD), and Brunauer-Emmett-Teller (BET) surface area analyzer.
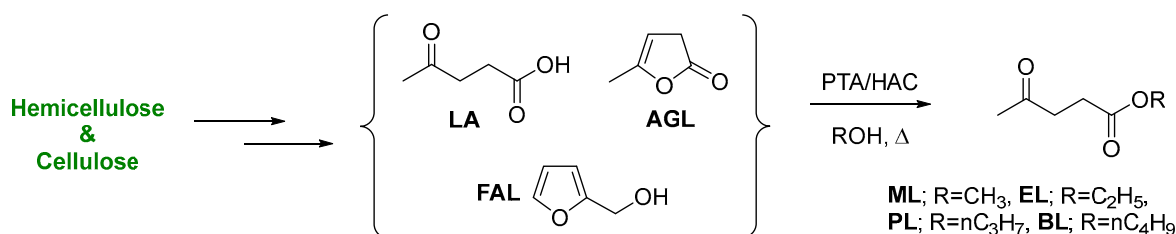
Scheme 1. Preparation of alkyl levulinates from levulinic acid and other chemical intermediates using phosphotungstic acid supported on humin-derived activated carbon as the acid catalyst.

2. Materials and Methods

2.1. Materials

Phosphotungstic acid hydrate was purchased from Sigma. HCl (aq., 35–38%) was purchased from Molychem. Xylose (99%), levulinic acid (LA, 98%), furfuryl alcohol (FAL, 98%), and benzyltributylammonium chloride (BTBAC, 99%) were procured from Spectrochem. n-Propanol (99.5%), n-butanol (99%), deionized (DI) water, 1,2-dichloroethane (DCE, 98%), orthophosphoric acid (85%) and sodium sulfate (anhydrous, 99%) were purchased from Loba Chemie Pvt. Ltd. Ethanol (99.9%) was procured from CSS. Methanol (99.9%) and chloroform (98%) were purchased from Finar. α-AGL was purchased from TCI. All the alcohols were used after drying over activated molecular sieves (4 Å) at room temperature for 12 h.

2.2. Preparation of Humin

Humin was obtained as the byproduct during the dehydration of xylose into FF in an aqueous-organic biphasic batch reaction setup [31]. In a round-bottomed glass pressure vessel fitted with a Teflon screw-top, xylose (2.00 g), HCl (20 mL, 20.2% aq.), DCE (20 mL), and BTBAC (10 wt.% of xylose) were introduced. The reactor was sealed and then placed in a preheated (100 °C) oil bath and stirred magnetically at 400 rpm for 3 h. The biphasic reaction mixture slowly turned from colorless to yellow to dark brown. After 3 h, the reactor was lifted from the oil bath and cooled in air. The reaction mixture was filtered through filter paper under a vacuum. The black solid residue (humin) collected on the filter paper was washed with DCE (25 mL) to remove soluble organic residues, followed by excess deionized water. The humin was dried in a hot-air oven for 24 h at 80 °C.

2.3. Preparation of HAC

Humin was chemically activated using H_3PO_4. In a typical process, 2 g of humin was mixed intimately with 85% H_3PO_4 (1:3, *w/w*) in a silica crucible and kept for 2 h. The mixture was carbonized at 500 and 600 °C in a muffle furnace for 2 h under N_2 flow. When the mixture was carbonized at 700 °C, it combusted partially, even under nitrogen flow. After carbonized mass (500 and 600 °C) was cooled to RT, suspended in deionized water (100 mL), and ultrasonicated for 30 min. The suspension was then filtered under a vacuum and repeatedly washed with deionized water until the pH of the filtrate increased to 7. The prepared samples were dried at 60 °C for 12 h in a hot-air oven and further sonicated

for 30 min in methanol for uniform dispersion. After removing methanol, the carbon was dried at 110 °C for 6 h, powdered in a mortar, and labeled as HAC-X, X corresponds to carbonization temperature.

2.4. Preparation of PTA/HAC-600 Catalyst

The catalyst was prepared by the incipient wetness impregnation method [32]. HAC-600 (0.4 g) was suspended in dry methanol (75 mL) and stirred for 30 min under room temperature. PTA (0.1 g) dissolved in methanol (10 mL) was added dropwise to the suspension under vigorous magnetic stirring, and the stirring was continued overnight at room temperature. After removing methanol under reduced pressure in a rotary evaporator, the catalyst was dried at 110 °C in a hot-air oven for 10 h.

2.5. Characterization Methods of Catalyst

The surface morphology of the samples was investigated using field-emission scanning electron microscopy (FESEM) in 7610FPLUS (Jeol, Akishima, Japan) and Gemini 300 Carl Zeiss, operating at an accelerating voltage of 15 kV. Powder X-ray diffraction (PXRD) spectra were recorded in a MiniFlex 600 (Rigaku, Tokyo, Japan) X-ray Powder Diffractometer using Cu Kα radiation as the source. Fourier-transform infrared spectroscopy (FTIR) of support and catalyst were recorded on a Bruker Alpha 400 FTIR spectrometer using the KBr pellet technique. The Brunauer–Emmett–Teller (BET) surface area of the samples was measured using Autosorb IQ-XR-XR, Anton Paar, employing N_2 adsorption at 77.35 K. The pore size distribution of the samples was determined from nitrogen desorption isotherms using the Barrett–Joyner–Halenda (BJH) method. The temperature-programmed desorption (TPD) measurement was performed using Quantachrome TPRWin v3.52 instrument. The sample was activated in helium gas with a flow rate of 30 mL min^{-1} at 200 °C for 110 min. After cooling, the sample was saturated with 10% NH_3 blended in He with a flow rate of 30 mL min^{-1} for 60 min. The analysis was carried out in the temperature range of 100–800 °C with a heating rate of 10 °C min^{-1}.

2.6. Catalytic Conversion of Biomass-Derived FAL, LA, and α-AGL to ALs

In a typical reaction, FAL (0.5 g), methanol (5 mL), and 20%PTA/HAC-600 (25 wt.%, 0.125 g) were charged into a 50 mL ACE glass pressure reactor fitted with a Teflon screw top and a magnetic stir bar. The glass pressure reactor was placed in a preheated oil bath (150 °C) and stirred magnetically for 7 h. After the reaction, the reactor was cooled to room temperature and opened. The excess methanol was evaporated in a rotary evaporator under reduced pressure. The leftover was then diluted in chloroform (20 mL) and the suspension was centrifuged to precipitate the catalyst. The catalyst was then washed with fresh chloroform (2 × 10 mL) and was then dried in a hot-air oven at 110 °C for 5 h before subjecting it to the next catalytic cycle. The chloroform solution was then evaporated in a rotary evaporator under reduced pressure to obtain the crude product. The crude product was chromatographed (silica gel, chloroform) to obtain pure ML (0.58 g, 87%) as a clear liquid. For FAL and LA, the reaction duration was 7 h. In the case of α-AGL, the reaction was worked up after 9 h.

3. Results

3.1. Physicochemical Characterization

The adsorption capacities of the synthesized HACs were determined by iodine number (IN) using ASTM D 4607-14R21 standards (Table 1) [33]. The IN of HAC-500 and 600 were calculated to be 727 mg/g and 853 mg/g, respectively. The textural characterization of the synthesized HACs was studied using nitrogen adsorption–desorption analysis, and the samples exhibited type IV adsorption isotherm. As observed from the BJH pore size distribution curves, the pore size ranged between 2 nm and 40 nm, and a distinct peak at 4.25 nm confirms that the materials are mesoporous with relatively uniform pore size distribution (Figure 1). HAC-600 was used for the catalyst preparation because of its higher

BET surface area than HAC-500 (Table 1). The high IN and BET surface area of HAC-600 makes it better catalyst support with a large micro- and mesoporous structure.

Table 1. Pore structure parameters of HAC-500, HAC-600, 20%PTA/HAC-500, and 20%PTA/HAC-600.

Sample	IN (mg/g)	S_{BET} (m²/g)	V_{total} (cc/g)	D_{avg} (nm)
HAC-500	727	1203	0.32	3.4
HAC-600	853	1425	0.33	2.8
20%PTA/HAC-500	-	937	0.11	3.4
20%PTA/HAC-600	-	947	0.12	2.5
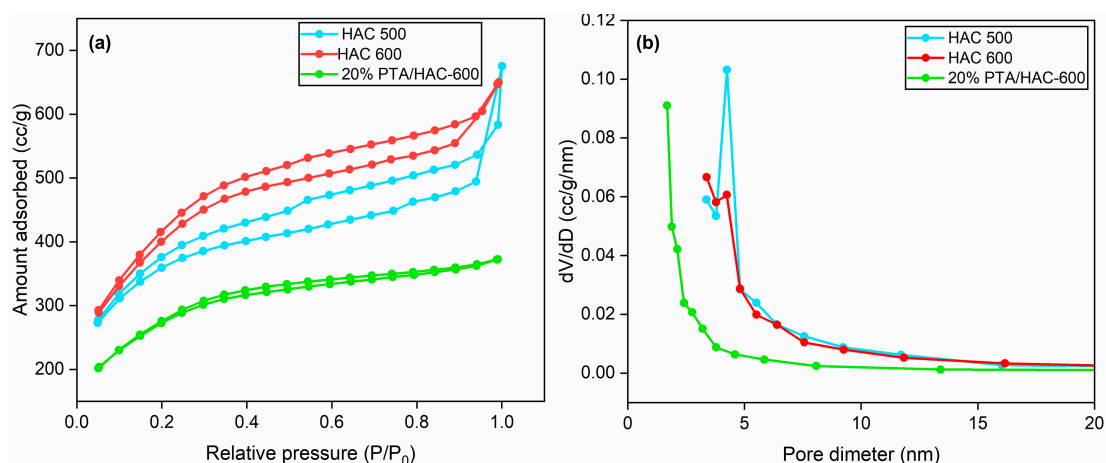
Figure 1. (**a**) N₂ adsorption isotherms and (**b**) BJH pore size distribution curves of HAC-500, HAC-600, and 20%PTA/HAC-600.

The surface morphology of the materials was determined using field-emission scanning electron microscopy (FESEM). The presence of constituent elements was confirmed by energy-dispersive X-ray analysis (EDAX) (Figure 2). The elemental mapping of the catalyst further confirmed the uniform distribution of the constituent elements.

The powder X-ray diffraction (PXRD) patterns of the HACs and catalyst are shown in Figure 3a. The scan was recorded in the 2θ range between 10–60°. A broad diffraction peak at 2θ = 23° confirms the amorphous nature of HAC. It is evident from the literature that peaks located at 2θ = 23° and 43° in HACs correspond to (002) and (101) planes of carbon. For PTA, peaks at 2θ = 10.8°, 18.3°, 23.5°, 25.6°, 29.9°, 35°, and 38.2° indicate the Keggin-type structure (JCPDS No. 50-0657). Distinct peaks of PTA are masked by the catalyst support (i.e., HAC) due to lower loading. The FTIR spectra of the HACs and the catalyst are shown in Figure 3b. The bands 2909 and 2838 cm⁻¹ correspond to C-H asymmetric and symmetric stretching, whereas bands assigned 1612 and 1392 cm⁻¹ correspond to C=C stretch and C-H bending vibrations. The peaks at 1079, 1020, 885, and 773 cm⁻¹ correspond to P-O_a, W=O_t, W-O_c-W, and W-O_e-W vibrational frequencies. The O_a, O_t, O_c, and O_e atoms represent the internal, terminal, corner, and edge-shared oxygen atoms. The NH₃-TPD profile for the catalyst is shown in Figure 4. Based on the temperature at which adsorbed ammonia molecules desorb, acidic sites in catalysts can be divided into several groups. Weak acidic sites desorb ammonia around 200–300 °C, moderate acidic sites around 300–450 °C, and strong acidic sites above 450 °C. From Figure 4, it is evident that the catalyst possesses weak and moderate acidic sites. The total acidity of the catalyst is calculated to be 1.7 mmol/g.

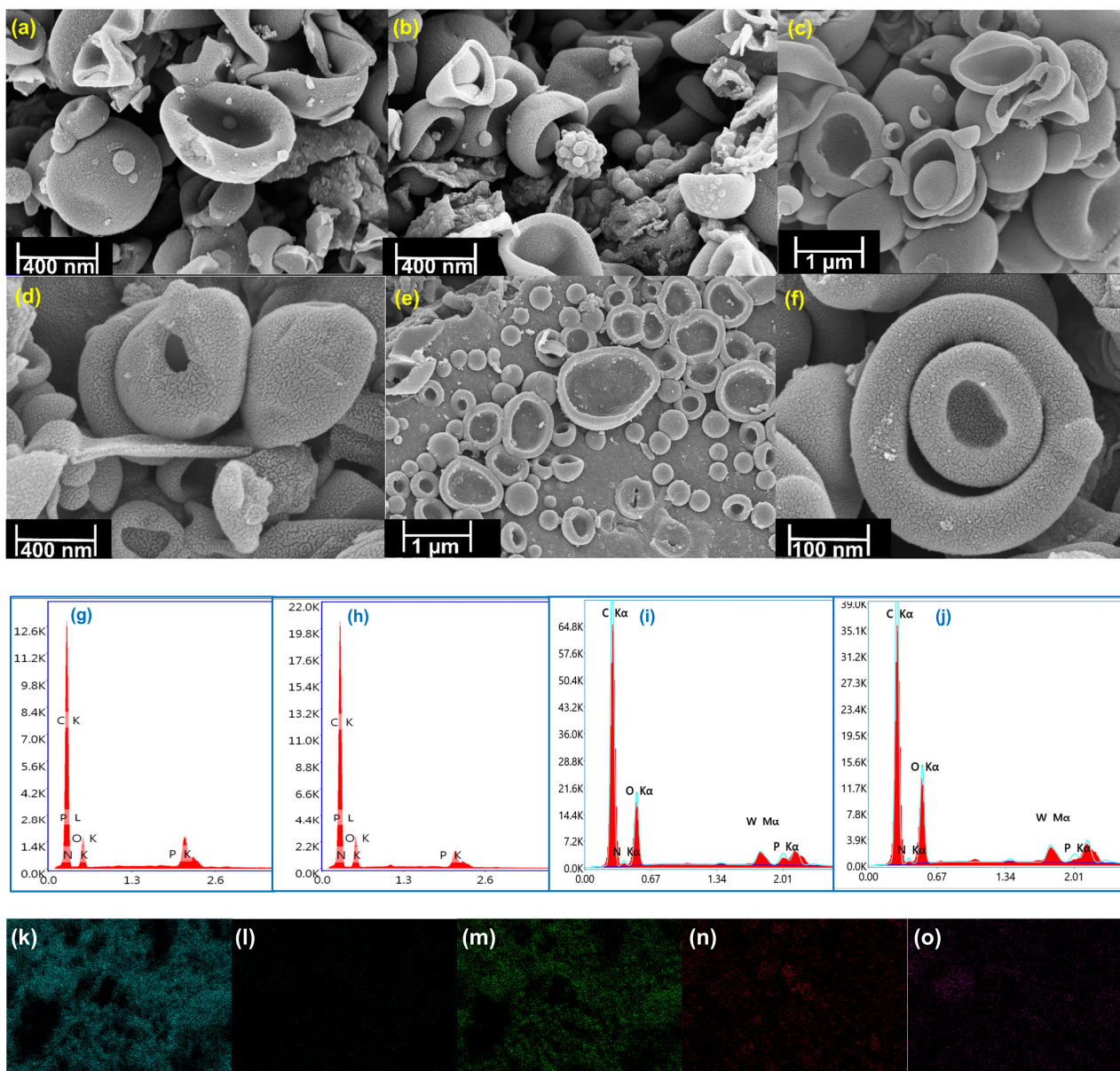**Figure 2.** FESEM images of (**a**) HAC-500, (**b**) HAC-600, (**c**,**d**) 20%PTA/HAC-600, and (**e**,**f**) 20%PTA/HAC-600 recycled after the fifth cycle; EDAX pattern of (**g**) HAC-500, (**h**) HAC-600, and (**i**) 20%PTA/HAC-600, and (**j**) 20%PTA/HAC-600 recycled after the fifth cycle; Elemental mapping of catalyst (**k**) C, (**l**) N, (**m**) O, (**n**) W, and (**o**) P.
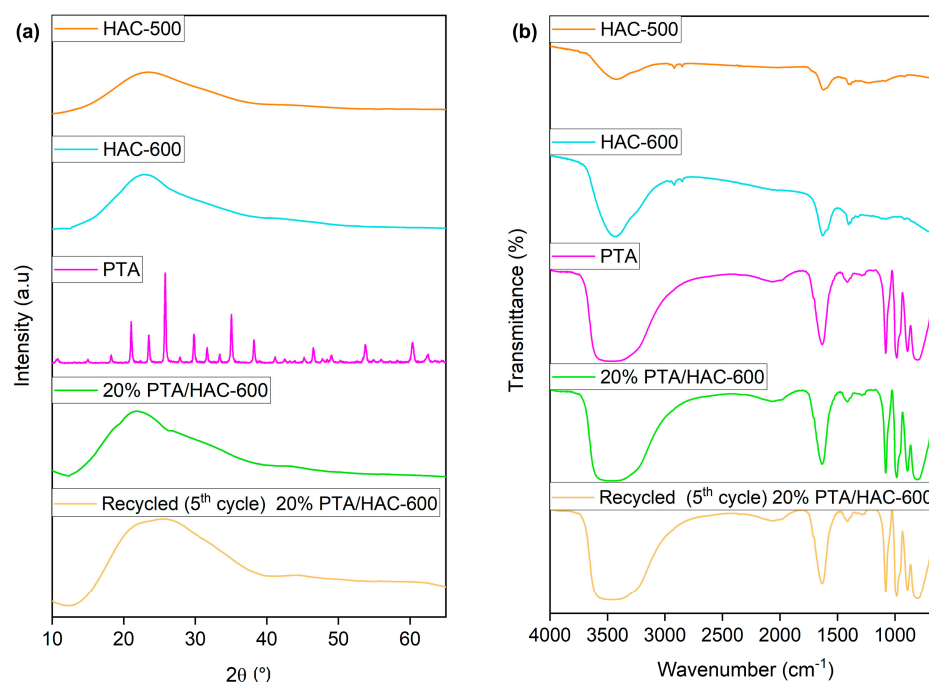
Figure 3. (**a**) PXRD patterns, and (**b**) FTIR spectra of HAC-500, HAC-600, PTA, 20%PTA/HAC-600, and recycled (5th cycle) 20%PTA/HAC-600.
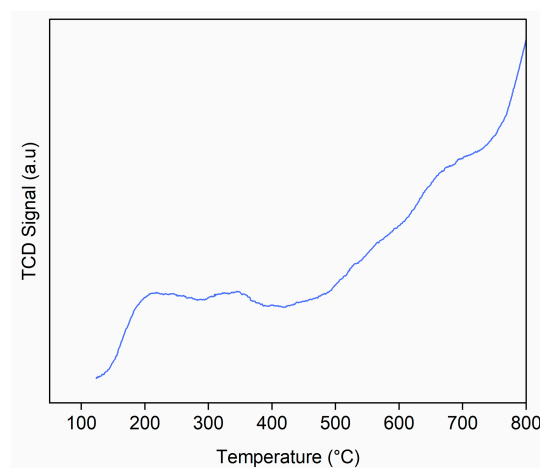

Figure 4. NH$_3$-TPD pattern of the 20%PTA/HAC-600 catalyst.

3.2. Catalytic Tests

The catalytic activity of the prepared 20%PTA/HAC-600 catalyst was evaluated towards the alcoholysis of FAL using excess methanol at 150 °C for the synthesis of methyl levulinate (ML). Firstly, the catalytic activity of 20%PTA/HAC-600 was compared with unsupported PTA and HAC-600. The use of the same amount of PTA (in comparison with PTA/HAC-600) gave only a 25% yield of ML, and in the case of HAC-600, no conversion of FAL to ML was observed under identical reaction conditions (150 °C, 7 h). The results can be explained by the rapid decomposition of FAL in the presence of homogeneous PTA. Since HAC has no significant acidic sites, it failed to catalyze the methanolysis of FAL. Furthermore, the effect of reaction parameters such as temperature, time, and catalyst loadings on the yield of ML was studied using FAL as a model substrate. All the reactions were performed in triplicate, and the average yields of isolated and spectroscopically pure ALs are reported (Figures S4–S15, SM). The yield variation between the trials was only 2–3%.

Temperature is one of the profound reaction parameters which affect the conversion and yield of the reaction. When the reaction was carried out at lower temperatures

(<150 °C), only moderate yields of ML (<70%) were obtained due to incomplete conversion of FAL (Figure 5). Quantitative conversion of FAL was ensured when the reaction was performed in a batch-type glass pressure reactor for 7 h at 150 °C, affording an 87% isolated yield of ML. However, further increasing the reaction temperature to 160 °C lowered the yield of ML due to the accelerated decomposition of FAL and also ML.
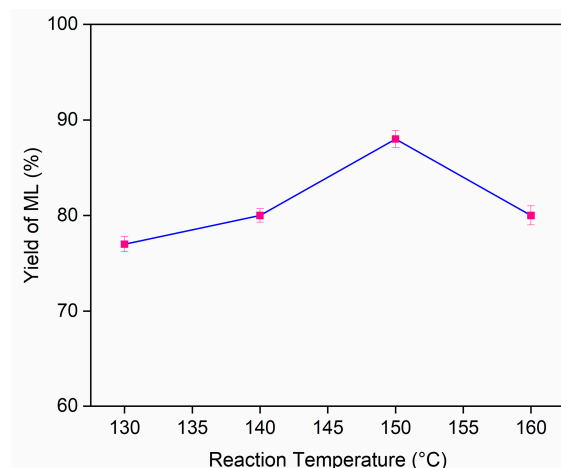

Figure 5. Effect of reaction temperature on the yield of ML. Reaction conditions: FAL (0.5 g, 5.09 mmol), methanol (5 mL), 20%PTA/HAC-600 (25 wt.%, 0.125 g), 7 h.

The effect of reaction duration was studied by varying the time between 5–8 h (Figure 6a). When the reaction was conducted for 7 h, ML was obtained in an 87% isolated yield with the quantitative conversion of FAL. No perceptible increase in the yield of ML was observed by prolonging the reaction time to 8 h. However, lowering the duration to 6 h decreased the isolated yield of ML to 75%. The result may be explained by the incomplete conversion of FAL in 6 h. The catalyst loading was varied from 10 wt.% to 30 wt.% to see its influence on the yield of ML (Figure 6b). Lower catalyst loadings (ca. 10 wt.%) resulted in the low conversion of FAL owing to the slow kinetics resulting from low concentration of acid sites catalyzing the transformation. A quantitative conversion of FAL with an 87% isolated yield of ML was obtained at 25 wt.% loading of 20%PTA/HAC-600. A further increase in the catalyst loading to 30 wt.% resulted in only a marginal increase (ca. 89%) in ML yield.
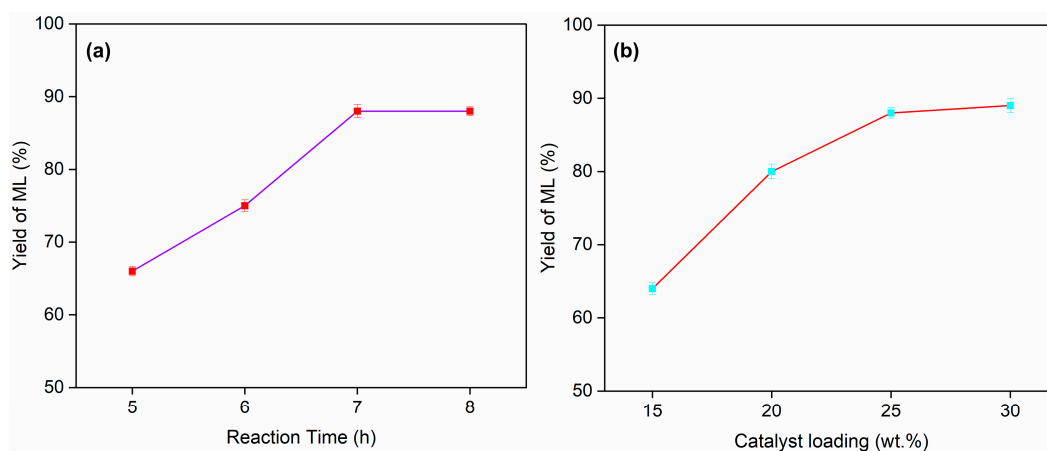

Figure 6. (**a**) Effect of reaction time on ML yield [Reaction conditions: FAL (0.5 g, 5.09 mmol), methanol (5 mL), 20%PTA/HAC-600 (25 wt.%, 0.125 g), 150 °C], and (**b**) Effect of catalyst loading [Reaction conditions: FAL (0.5 g, 5.09 mmol), methanol (5 mL), 150 °C, 7 h] on the yield of ML.

Therefore, a maximum of 87% of ML was isolated with the quantitative conversion of FAL under optimized reaction conditions (150 °C, 7 h, 25 wt.% of 20%PTA/HAC-600). The same optimized reaction conditions were applied for the synthesis of alkyl levulinates (ALs) using C1-C4 alcohols (Table 2). Under identical reaction conditions, ethyl levulinate (EL), propyl levulinate (PL), and butyl levulinate (BL) were isolated in 85%, 83%, and 85% yield, respectively, using 20%PTA/HAC-600 as a heterogeneous acid catalyst.

Table 2. Conversion of furfuryl alcohol to alkyl levulinates.

Entry	Product	Yield (%)
1	ML	87
2	EL	85
3	PL	83
4	BL	85

Reaction conditions: FAL (0.5 g, 5.09 mmol), alcohol (5 mL), 20%PTA/HAC-600 (25 wt.%, 0.125 g), 150 °C, 7 h.

We envisaged that the synthetic protocol would work equally well for synthesizing ALs starting from biomass-derived intermediates, such as LA and α-AGL, under optimized reaction conditions. Esterification of LA with n-propanol provided PL in a 90% isolated yield, whereas methanol, ethanol, and n-butanol gave 85%, 88%, and 87% of ML, EL, and BL, respectively (Table 3).

Table 3. Conversion of levulinic acid to alkyl levulinates.

Entry	Product	Yield (%)
1	ML	85
2	EL	88
3	PL	90
4	BL	87

Reaction conditions: LA (0.5 g, 4.30 mmol), alcohol (5 mL), 20%PTA/HAC-600 (25 wt.%, 0.125 g), 150 °C, 7 h.

Similarly, the same protocol was extended for the synthesis of ALs from α-AGL using C1–C4 alcohols (Table 4). When the reaction was carried out using methanol, 91% of ML was isolated. The use of ethanol provided 84% of EL, whereas n-propanol and n-butanol resulted in 86% PL and 88% BL, respectively, starting from α-AGL when the reactions were performed at 150 °C for 9 h using 20%PTA/HAC-600 (25 wt.% of α-AGL) catalyst.

Table 4. Conversion of α-angelica lactone to alkyl levulinates.

Entry	Product	Yield (%)
1	ML	91
2	EL	84
3	PL	86
4	BL	88

Reaction conditions: α-AGL (0.5 g, 5.09 mmol), alcohol (5 mL), 20%PTA/HAC-600 (25 wt.%, 0.125 g), 150 °C, 9 h.

Similarly, the 20%PTA/HAC-500 catalyst was synthesized and characterized (Figures S1–S3, SM). The catalytic tests were further carried out using a 20%PTA/HAC-500 catalyst for the alcoholysis of FAL using C1–C4 alcohols, and the results were compared with a 20%PTA/HAC-600 catalyst. A marginal decrease in the yields of ALs was only observed using a 20%PTA/HAC-500 catalyst. Under optimized reaction conditions, ML was obtained in 85% yield, whereas EL, PL, and BL were obtained in 85, 82, and 83% yields, respectively (Figure 7). The results may be explained by the better adsorption of PTA on HAC-600 when compared to HAC-500 due to better porosity and higher surface area of the former supporting material.
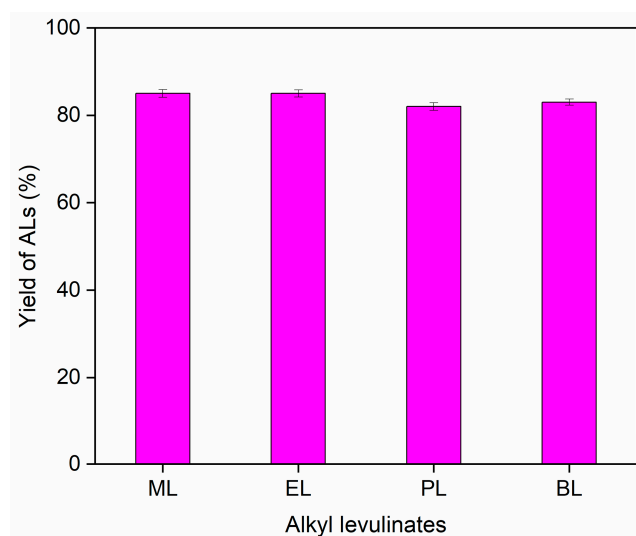
Figure 7. Conversion of FAL to various ALs using 20%PTA/HAC-500 catalyst. Reaction conditions: FAL (0.5 g, 5.09 mmol), alcohol (5 mL), 20%PTA/HAC-500 (25 wt.%, 0.125 g), 7 h.

3.3. Catalyst Recyclability

The recyclability of the 20%PTA/HAC-600 catalyst used for transforming FAL into ML was studied (Figure 8). The trials were carried out under optimized reaction conditions (0.5 g FAL, 150 °C, 7 h, 25 wt.% catalyst, 5 mL methanol). After the reaction, the volatiles (i.e., excess methanol) were removed from the mixture under reduced pressure. The catalyst was centrifuged and washed with chloroform. The catalyst was dried at 110 °C for 5 h before using it in the next catalytic cycle. The catalyst was successfully recycled for five consecutive cycles with good conversion and selectivity towards ML. Since there was minor mass loss during the catalyst recovery, the starting amount of FAL was adjusted accordingly for consistency of catalyst loading in consecutive cycles. Up to the third cycle, the loss in yield of ML was nominal, whereas the fourth and fifth cycles showed a noticeable loss in yield.
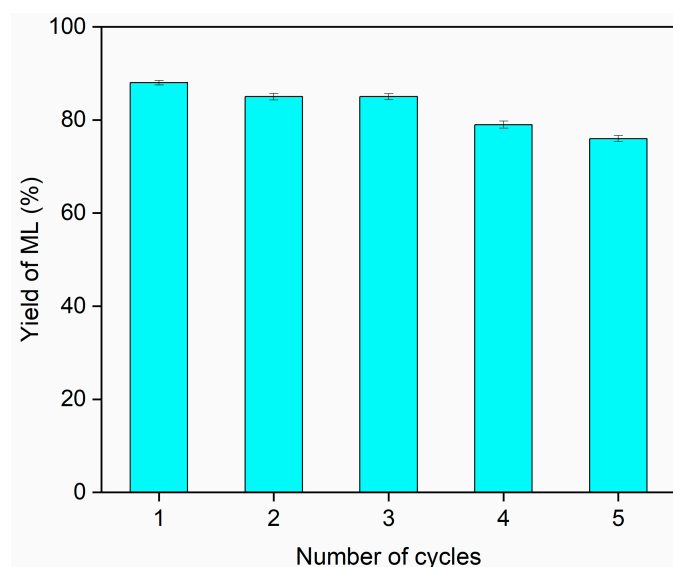

Figure 8. Catalyst recyclability test for the conversion of FAL to ML. Reaction conditions: FAL (0.5 g, 5.09 mmol), methanol (5 mL), 20%PTA/HAC-600 (25 wt.%, 0.125 g), 150 °C, 7 h.

Whereas the fresh 20%PTA/HAC-600 catalyst afforded an 87% yield of ML, the catalyst at the fifth consecutive cycle produced ML in a 76% yield. The marginal loss in the yield

of ML can be the slight leaching of PTA from the HAC-600 support, which is a common occurrence in supported acid catalysts. The catalyst recyclability was also examined for esterifying LA with alkyl alcohols. The process is more challenging since water is formed as a byproduct, which may lead to increased leaching of PTA from the HAC-600 support. As predicted, the fresh catalyst provided an 88% yield of EL from LA, which decreased to 62% after the third catalytic cycle (Figure S16, SM). However, the prior evaporation of polar volatiles (i.e., ethanol, water) before separating the catalyst assists in redepositing the leached PTA back into the HAC-600 support.

4. Conclusions

Humin worked as a promising feedstock for deriving activated carbon with high surface area with micro- and mesoporosity. HAC was successfully used as a supporting material for PTA to produce a heterogeneous acid catalyst. The 20%PTA/HAC-600 catalyst produced alkyl levulinates in good to excellent isolated yields starting from carbohydrate-derived chemical intermediates, such as LA, FAL, and α-AGL. The catalyst was successfully recovered and recycled for five catalytic cycles. This work will create interest in the high-value application of humin, a waste product produced in the biorefinery. Future work will explore the efficiency of the PTA/HAC-600 catalyst towards other acid-catalyzed reactions for the catalytic value addition of biomass and sustainable organic synthesis in general.

Supplementary Materials: The following supporting information can be downloaded at: https://www.mdpi.com/article/10.3390/chemistry5020057/s1, Figure S1. FESEM images of 20%PTA/HAC-500; Figure S2. (a) EDAX pattern, and (b) PXRD pattern of 20%PTA/HAC-500; Figure S3. (a) IR spectrum, (b) N2 adsorption isotherm, and BJH pore size distribution curve (inset) of 20%PTA/HAC-500; Figure S4. The FTIR spectrum of methyl levulinate; Figure S5. The 1H-NMR spectrum of methyl levulinate; Figure S6. The 13C-NMR spectrum of methyl levulinate; Figure S7. The FTIR spectrum of ethyl levulinate; Figure S8. The 1H-NMR spectrum of ethyl levulinate; Figure S9. The 13C-NMR spectrum of ethyl levulinate; Figure S10. The FTIR spectrum of propyl levulinate; Figure S11. The 1H-NMR spectrum of propyl levulinate; Figure S12. The 13C-NMR spectrum of propyl levulinate; Figure S13. The FTIR spectrum of butyl levulinate; Figure S14. The 1H-NMR spectrum of butyl levulinate; Figure S15. The 13C-NMR spectrum of butyl levulinate; Figure S16. Catalyst recyclability test for the conversion of LA to EL.

Abbreviations

α-AGL	α-Angelica lactone
HAC	Humin-derived activated carbon
AL	Alkyl levulinate
ML	Methyl levulinate

LA	Levulinic acid
FF	Furfural
FAL	Furfuryl alcohol
EL	Ethyl levulinate
PL	Propyl levulinate
BL	Butyl levulinate
HPA	Heteropoly acid
PTA	Phosphotungstic acid

References

1. Ubando, A.T.; Felix, C.B.; Chen, W.-H. Biorefineries in Circular Bioeconomy: A Comprehensive Review. *Bioresour. Technol.* **2020**, *299*, 122585. [CrossRef] [PubMed]
2. Deng, W.; Feng, Y.; Fu, J.; Guo, H.; Guo, Y.; Han, B.; Jiang, Z.; Kong, L.; Li, C.; Liu, H.; et al. Catalytic Conversion of Lignocellulosic Biomass into Chemicals and Fuels. *Green Energy Environ.* **2023**, *8*, 10–114. [CrossRef]
3. Alonso, D.M.; Bond, J.Q.; Dumesic, J.A. Catalytic Conversion of Biomass to Biofuels. *Green Chem.* **2010**, *12*, 1493–1513. [CrossRef]
4. Vassilev, S.V.; Vassileva, C.G. Composition, Properties and Challenges of Algae Biomass for Biofuel Application: An Overview. *Fuel* **2016**, *181*, 1–33. [CrossRef]
5. Jérôme, F.; De Oliveira Vigier, K. Catalytic Conversion of Carbohydrates to Furanic Derivatives in the Presence of Choline Chloride. *Catalysts* **2017**, *7*, 218. [CrossRef]
6. Bhaumik, P.; Dhepe, P.L. Solid Acid Catalyzed Synthesis of Furans from Carbohydrates. *Catal. Rev.* **2016**, *58*, 36–112. [CrossRef]
7. Zhao, Y.; Lu, K.; Xu, H.; Zhu, L.; Wang, S. A Critical Review of Recent Advances in the Production of Furfural and 5-Hydroxymethylfurfural from Lignocellulosic Biomass through Homogeneous Catalytic Hydrothermal Conversion. *Renew. Sustain. Energy Rev.* **2021**, *139*, 110706. [CrossRef]
8. Mariscal, R.; Maireles-Torres, P.; Ojeda, M.; Sádaba, I.; Granados, M.L. Furfural: A Renewable and Versatile Platform Molecule for the Synthesis of Chemicals and Fuels. *Energy Environ. Sci.* **2016**, *9*, 1144–1189. [CrossRef]
9. Eseyin, A.E.; Steele, P.H. An Overview of the Applications of Furfural and Its Derivatives. *Int. J. Adv. Chem.* **2015**, *3*, 42–47. [CrossRef]
10. Xu, C.; Paone, E.; Rodríguez-Padrón, D.; Luque, R.; Mauriello, F. Recent Catalytic Routes for the Preparation and the Upgrading of Biomass Derived Furfural and 5-Hydroxymethylfurfural. *Chem. Soc. Rev.* **2020**, *49*, 4273–4306. [CrossRef]
11. Dusselier, M.; Mascal, M.; Sels, B.F. Top Chemical Opportunities from Carbohydrate Biomass: A Chemist's View of the Biorefinery. In *Selective Catalysis for Renewable Feedstocks and Chemicals*; Nicholas, K.M., Ed.; Topics in Current Chemistry; Springer International Publishing: Cham, Switzerland, 2014; Volume 353, pp. 1–40. ISBN 978-3-319-08653-8.
12. Tian, Y.; Zhang, F.; Wang, J.; Cao, L.; Han, Q. A Review on Solid Acid Catalysis for Sustainable Production of Levulinic Acid and Levulinate Esters from Biomass Derivatives. *Bioresour. Technol.* **2021**, *342*, 125977. [CrossRef]
13. Dutta, S.; Bhat, N.S. Recent Advances in the Value Addition of Biomass-Derived Levulinic Acid: A Review Focusing on Its Chemical Reactivity Patterns. *ChemCatChem* **2021**, *13*, 3202–3222. [CrossRef]
14. Hayes, D.J.; Fitzpatrick, S.; Hayes, M.H.B.; Ross, J.R.H. The Biofine Process– Production of Levulinic Acid, Furfural, and Formic Acid from Lignocellulosic Feedstocks. In *Biorefineries-Industrial Processes and Products*; Kamm, B., Gruber, P.R., Kamm, M., Eds.; Wiley-VCH Verlag GmbH: Weinheim, Germany, 2005; pp. 139–164. ISBN 978-3-527-61984-9.
15. Di Bucchianico, D.D.M.; Wang, Y.; Buvat, J.-C.; Pan, Y.; Moreno, V.C.; Leveneur, S. Production of Levulinic Acid and Alkyl Levulinates: A Process Insight. *Green Chem.* **2022**, *24*, 614–646. [CrossRef]
16. Démolis, A.; Essayem, N.; Rataboul, F. Synthesis and Applications of Alkyl Levulinates. *ACS Sustain. Chem. Eng.* **2014**, *2*, 1338–1352. [CrossRef]
17. Ahmad, K.A.; Siddiqui, M.H.; Alam, M.I.; Haider, M.A.; Ahmad, E. Keggin Heteropolyacid Catalysts: Synthesis, Heterogenization, and Application in Conversion of Biomass-Derived Molecules. In *Catalysis*; Spivey, J., Han, Y.-F., Shekhawat, D., Eds.; Royal Society of Chemistry: Cambridge, UK, 2022; Volume 34, pp. 206–247. ISBN 978-1-83916-499-6.
18. Zhang, Q.; Luo, Q.; Wu, Y.; Yu, R.; Cheng, J.; Zhang, Y. Construction of a Keggin Heteropolyacid/Ni-MOF Catalyst for Esterification of Fatty Acids. *RSC Adv.* **2021**, *11*, 33416–33424. [CrossRef] [PubMed]
19. Gao, Z.; Zhou, Z.; Wang, M.; Shang, N.; Gao, W.; Cheng, X.; Gao, S.; Gao, Y.; Wang, C. Highly Dispersed Pd Anchored on Heteropolyacid Modified ZrO_2 for High Efficient Hydrodeoxygenation of Lignin-Derivatives. *Fuel* **2023**, *334*, 126768. [CrossRef]
20. Luo, X.; Wu, H.; Li, C.; Li, Z.; Li, H.; Zhang, H.; Li, Y.; Su, Y.; Yang, S. Heteropoly Acid-Based Catalysts for Hydrolytic Depolymerization of Cellulosic Biomass. *Front. Chem.* **2020**, *8*, 580146. [CrossRef]
21. Bhat, N.S.; Mal, S.S.; Dutta, S. Recent Advances in the Preparation of Levulinic Esters from Biomass-Derived Furanic and Levulinic Chemical Platforms Using Heteropoly Acid (HPA) Catalysts. *Mol. Catal.* **2021**, *505*, 111484. [CrossRef]
22. Wu, Y.; Ye, X.; Yang, X.; Wang, X.; Chu, W.; Hu, Y. Heterogenization of Heteropolyacids: A General Discussion on the Preparation of Supported Acid Catalysts. *Ind. Eng. Chem. Res.* **1996**, *35*, 2546–2560. [CrossRef]
23. Lam, E.; Luong, J.H.T. Carbon Materials as Catalyst Supports and Catalysts in the Transformation of Biomass to Fuels and Chemicals. *ACS Catal.* **2014**, *4*, 3393–3410. [CrossRef]

24. Lin, Y.; Yu, J.; Zhang, X.; Fang, J.; Lu, G.-P.; Huang, H. Carbohydrate-Derived Porous Carbon Materials: An Ideal Platform for Green Organic Synthesis. *Chin. Chem. Lett.* **2022**, *33*, 186–196. [CrossRef]

25. Ayashi, N.; Chermahini, A.N.; Saraji, M. Biomass Conversion to Alkyl Levulinates Using Heteropoly Acid Carbon Mesoporous Composites. *Process Saf. Environ. Prot.* **2022**, *160*, 988–1000. [CrossRef]

26. Chhabra, T.; Rohilla, J.; Krishnan, V. Nanoarchitectonics of Phosphomolybdic Acid Supported on Activated Charcoal for Selective Conversion of Furfuryl Alcohol and Levulinic Acid to Alkyl Levulinates. *Mol. Catal.* **2022**, *519*, 112135. [CrossRef]

27. Patil, S.K.R.; Heltzel, J.; Lund, C.R.F. Comparison of Structural Features of Humins Formed Catalytically from Glucose, Fructose, and 5-Hydroxymethylfurfuraldehyde. *Energy Fuels* **2012**, *26*, 5281–5293. [CrossRef]

28. Xu, Z.; Yang, Y.; Yan, P.; Xia, Z.; Liu, X.; Zhang, Z.C. Mechanistic Understanding of Humin Formation in the Conversion of Glucose and Fructose to 5-Hydroxymethylfurfural in [BMIM]Cl Ionic Liquid. *RSC Adv.* **2020**, *10*, 34732–34737. [CrossRef] [PubMed]

29. Liu, S.; Zhu, Y.; Liao, Y.; Wang, H.; Liu, Q.; Ma, L.; Wang, C. Advances in Understanding the Humins: Formation, Prevention and Application. *Appl. Energy Combust. Sci.* **2022**, *10*, 100062. [CrossRef]

30. Yang, J.; Niu, X.; Wu, H.; Zhang, H.; Ao, Z.; Zhang, S. Valorization of Humin as a Glucose Derivative to Fabricate a Porous Carbon Catalyst for Esterification and Hydroxyalkylation/Alkylation. *Waste Manag.* **2020**, *103*, 407–415. [CrossRef]

31. Bhat, N.S.; Vinod, N.; Onkarappa, S.B.; Dutta, S. Hydrochloric Acid-Catalyzed Coproduction of Furfural and 5-(Chloromethyl)furfural Assisted by a Phase Transfer Catalyst. *Carbohydr. Res.* **2020**, *496*, 108105. [CrossRef]

32. Kozhevnikov, I.V.; Kloetstra, K.R.; Sinnema, A.; Zandbergen, H.W.; van Bekkum, H. Study of Catalysts Comprising Heteropoly Acid $H_3PW_{12}O_{40}$ Supported on MCM-41 Molecular Sieve and Amorphous Silica. *J. Mol. Catal. A Chem.* **1996**, *114*, 287–298. [CrossRef]

33. *ASTM D4607-14R21*; Standard Test Method for Determination of Iodine Number of Activated Carbon. ASTM International: West Conshohocken, PA, USA, 2021. [CrossRef]